



RESEARCH ARTICLE

Shifting brain circuits in pain chronicity

Andrew M. Youssef^{1,2}  | Monica Azqueta-Gavaldon^{3,4} | Katie E. Silva^{1,2} |
 Nadia Barakat^{1,2} | Natalia Lopez^{1,2} | Farah Mahmud^{1,2} | Alyssa Lebel^{1,2} |
 Navil F. Sethna^{1,2} | David Zurakowski^{1,2} | Laura E. Simons⁵ | Eduard Kraft^{3,4} |
 David Borsook^{1,2} 

¹Center for Pain and the Brain, Department of Anesthesiology, Critical Care and Pain Medicine, Boston Children's Hospital, Boston, Massachusetts

²Department of Anesthesia, Harvard Medical School, Boston, Massachusetts

³Department of Orthopedics, Physical Medicine and Rehabilitation, Medical Centre of University of Munich, Munich, Germany

⁴Interdisciplinary Pain Unit, Medical Centre of University of Munich, Munich, Germany

⁵Department of Anesthesiology, Perioperative and Pain Medicine, Stanford University School of Medicine, Stanford, California

Correspondence

David Borsook, MD, PhD, Center for Pain and the Brain, c/o 1 Autumn Street, Boston Children's Hospital, Harvard Medical School, Boston MA.

Email: david.borsook@childrens.harvard.edu

Funding information

Mayday Fund; National Institute of Health, Grant/Award Numbers: K23HD067202, K24NS064050, R01NS065051

Abstract

The evaluation of brain changes to a specific pain condition in pediatric and adult patients allows for insights into potential mechanisms of pain chronicity and possibly long-term brain changes. Here we focused on the primary somatosensory system (SS) involved in pain processing, namely the ventroposterolateral thalamus (VPL) and the primary somatosensory cortex (SI). We evaluated, using MRI, three specific processes: (a) somatotopy of changes in the SS for different pain origins (viz., foot vs. arm); (b) differences in acute (ankle sprain versus complex regional pain syndrome-CRPS); and (c) differences of the effects of CRPS on SS in pediatric versus adult patients. In all cases, age- and sex-matched individuals were used as controls. Our results suggest a shift in concurrent gray matter density (GMD) and resting functional connectivity strengths (rFC) across pediatric and adult CRPS with (a) differential patterns of GMD (VPL) and rFC (SI) on SS in pediatric vs. adult patterns that are consistent with upper and lower limb somatotopical organization; and (b) widespread GMD alterations in pediatric CRPS from sensory, emotional and descending modulatory processes to more confined sensory-emotional changes in adult CRPS and rFC patterns from sensory-sensory alterations in pediatric populations to a sensory-emotional change in adult populations. These results support the idea that pediatric and adult CRPS are differentially represented and may reflect underlying differences in pain chronification across age groups that may contribute to the well-known differences between child and adult pain vulnerability and resilience.

KEYWORDS

adult, arm, brain, complex regional pain, CRPS, leg, nerve, pediatric, S1, thalamus

1 | INTRODUCTION

Evaluation of chronic pain across pediatric and adult populations, even for the same disease, is difficult to study. Complex regional pain syndrome (CRPS) is a chronic pain condition that is observed in both age groups. CRPS is a disease that usually begins with a peripheral injury and results in multiple brain changes. Spread of pain (van Rijn et al.,

2011), inattention (Bultitude, Walker, & Spence, 2017), movement disorders (Verdugo & Ochoa, 2000), neglect-like symptoms (Maihofner & Birklein, 2007) make this a notable pain disease that afflicts multiple brain systems. While this condition may extend into adulthood, studies comparing the differences in how the brain responds to a peripheral nerve injury (most common cause [Low, Ward, & Wines, 2007]) have not been well described.

Compared with pain-free controls, pediatric CRPS patients are associated with wide-spread brain gray matter atrophy in motor, affective, motivational, emotional, cognitive, memory, and fear-related regions (Erpelding et al., 2016), whereas atrophy in adults appears to be more confined to affective, motivational and cognitive regions (Barad, Ueno, Younger, Chatterjee, & Mackey, 2014; Geha et al., 2008). Additionally, more apparent, are the mixed reports in child and adult populations across resting functional connectivity metrics between brain signal covariation and within brain networks (such as the default mode network). Indeed, in our recent pediatric investigations, we have reported hyperconnectivity patterns in neural networks (Becerra et al., 2014) and amygdala-based covariation (Simons et al., 2014), whereas adult patients are associated with wide-spread hypoconnectivity patterns in the default mode network (Bolwerk, Seifert, & Maihofner, 2013) and insula-centered covariation (Kim, Choi, et al., 2017).

CRPS caused by peripheral nerve injury provides a unique opportunity to investigate specific brain processes involved in disease progression, such as somatotopic specificity of somatosensory changes; chronicity of changes and plasticity of responsivity (resilience to treatment/resistance to disease reversal). While there is a clear distinction in structural and functional metrics across aging populations, it is possible that the reported differential changes in pediatric versus adult CRPS patients reflect age-related effects, or perhaps a transition of circuitry as a consequence of disease duration. Indeed, it is possible that there is a shift from sensory to emotional circuits with pain chronification (Hashmi et al., 2013). However, while this shift is evident in adult populations, it remains unclear whether a similar cascade is present across pediatric and young adult groups. In any case, while differences between patients with CRPS are reported relative to healthy controls, it remains unknown whether a similar set of brain morphometry and resting connectivity circuits are involved during the acute phase of the disease. Furthermore, the relative contribution of the affected limb remains uncertain, as no study to date reports altered structural metrics within brain sites with fine discriminatory somatotopic representations, notably the primary somatosensory cortex (Penfield & Boldrey, 1937) and the ventral posterior thalamic nucleus (Kaas, Nelson, Sur, Dykes, & Merzenich, 1984).

We employed magnetic resonance imaging (MRI) techniques to determine potential brain structural (gray matter density) and subsequent resting functional connectivity strengths in acute (ankle sprain) and chronic (CRPS) pain affecting the leg in pediatric patients and between controls to determine effects of pain "evolution" affecting the same body region. In addition, we evaluated the same metrics in adult chronic (CRPS) pain patients vs. healthy controls affecting the arm to determine the regional somatotopy in sensory regions (viz., thalamus and sensory cortex), as well as to ascertain whether or not if the adult CRPS brain responds differently when compared to the pediatric CRPS brain. Based on previous findings described above, our hypotheses were: (a) alterations within the ventral postero-lateral (VPL) thalamic nucleus or primary somatosensory (SI) cortex should correspond to upper or lower limb somatotopical organization, which would define the specificity of other observed changes; (b) these

somatosensory regions would show gray matter atrophy and functional hyperconnectivity patterns in chronic pain patients vs. matched controls in both pediatric and adult patients affecting the same body region; (c) in comparing acute vs. chronic pain cohorts (matched for age and sex) with pain affecting the same body region, the acute group will display less robust gray matter and functional alterations based on the duration of the disease.

2 | MATERIALS AND METHODS

2.1 | Subjects

Fifty-two patients and 52 healthy controls (matched for sex and age) were recruited for the study. The patient group consisted of 32 pediatric patients, equally distributed with unilateral acute or chronic pain of the lower limb extremity (acute, 10 females, 6 males, mean \pm SEM age: 15.8 ± 0.6 years, range 11–22 years; chronic, 10 females, 6 males, age: 14.3 ± 0.6 years, range 10–17 years; controls, 20 females, 12 males, age: 15 ± 2.7 years, range 10–20 years) and 20 adult patients with unilateral chronic pain of the upper limb extremity (chronic, 15 females, 5 males, age: 57.9 ± 9 years, range 37–71 years; controls, 15 females, 5 males, age: 58.5 ± 10 years, range 37–73 years). Within both the adult and the pediatric patients, there were no significant group differences in age (two-sample *t*-test; $p > .05$) or sex composition (chi-square test, $p > .05$). Here, it is pertinent to note that patients with acute pain were recruited are part of an ongoing longitudinal study, and although one subject slightly exceeded the 3-month reference point, recovery was within a week and as such, we considered it appropriate to include this subject in our acute sample. All chronic pain (3 months or greater) patients were diagnosed with CRPS Type I by Budapest criteria by an experienced pain neurologist (AL, DB) in accordance with a neurological examination and a comprehensive record review. Pediatric patients were recruited from the Pain Treatment Services, Emergency, Orthopedics, and Sports Medicine departments at Boston Children's Hospital. Adult patients were recruited from the Interdisciplinary Pain Unit and Medical Centre of University of Munich, as well as through two internet-based CRPS self-help network sites (crps-netwerk.org; unfallopfer.de). Individual patients reported their average pain intensity from the time of injury on a numerical rating scale (0 = no pain, 1–3 = mild pain, 4–6 = moderate pain, 7–10 = severe pain). Pediatric healthy controls were recruited through flyers on bulletin boards throughout the local community, online list serves (e.g., craigslist, college job boards) and word of mouth.

Participants were excluded from the study if they had any other neurological symptoms, severe medical problems (such as uncontrollable asthma and seizures, cardiac diseases or severe psychiatric disorders), medical implants and/or devices or weighed more than 285 pounds, corresponding to the MRI scanner weight limit. All patients were instructed not to take analgesic medication within at least 4 hr prior to the study scanning session. For the pediatric population, written informed consent and assent were obtained for all procedures, which were conducted under the approval of the Boston Children's Hospital Institutional Review Board. Written consent was

obtained for all procedures, which were conducted under the approval of the Ethics Committee of the Ludwig Maximilian University of Munich and met the Helsinki criteria for the study of pain in humans.

2.2 | MRI acquisition

All subjects were positioned supine in a Siemens 3 T MRI scanner. For image registration, a three-dimension magnetization-prepared rapid gradient-echo (MP-RAGE) sequence was used to acquire a high-resolution T1-weighted anatomical image (raw voxel size = 1.0 mm thick, matrix = 256 × 256 voxels). With the subject still at rest, a series of gradient echo echo-planar image sets with Blood Oxygen Level Dependent contrast were collected as follows: (a) Siemens Magnetom Trio 3 T (image series = 425, axial slices = 51, repetition time = 1,100 ms, echo time = 30 ms, raw voxel size = 3.00 × 3.00 × 3.00 mm thick, matrix = 76 × 76 voxels, 16 acute, 16 controls); (b) Siemens Magnetom Trio 3 T (image series = 150, axial slices = 41, repetition time = 3,000 ms, echo time = 35 ms, raw voxel size = 3.75 × 3.75 × 3.50 mm thick, matrix = 64 × 64 voxels, 8 pediatric chronic, 8 controls); (c) Siemens Magnetom Trio 3 T (image series = 200, axial slices = 41, repetition time = 2,500 ms, echo time = 35 ms, raw voxel size = 3.75 × 3.75 × 3.50 mm thick, matrix = 64 × 64 voxels, 8 pediatric chronic, 8 controls); (d) Siemens Magnetom Skyra 3 T (image series = 250, axial slices = 39, repetition time = 2,500 ms, echo time = 30 ms, raw voxel size = 3.50 × 3.50 × 3.85 mm thick, matrix = 64 × 64 voxels, 20 adult chronic pain, 20 controls). Note that all T1-weighted images were collected on the same scanner as the functional images, that is, as they were all collected on the same session.

2.3 | MRI analysis

2.3.1 | Gray matter density analysis

Using SPM12 (Friston et al., 1994), image preprocessing and gray matter density maps were created with the computational anatomy toolbox (dbm.neuro.uni-jena.de/cat). Here, prior to segmentation, all T1-weighted images in pediatric patients with unilateral left pain were flipped to the right (pediatric acute pain, $n = 7$; pediatric chronic pain; $n = 9$). All T1-weighted images were then segmented into gray matter (GM), white matter (WM), and cerebrospinal fluid (CSF) probability maps. Here, the segmentation approach was based on the Adaptive Maximum A-Posterior technique to model local variations and parameters as slowly varying spatial functions (Rajapakse, Giedd, & Rapoport, 1997) and the partial volume estimation method whereby the fraction of each tissue type within each voxel is estimated to yield more accurate segmentation (Tohka, Zijdenbos, & Evans, 2004). Furthermore, to enhance the quality of the T1-weighted images and further improve the segmentation, we combined two denoising methods: the Spatially Adaptive Non-Local Means (SANLM) filter (Manjon, Coupe, Marti-Bonmati, Collins, & Robles, 2010) and the classical Markov Random Field method (Rajapakse et al., 1997). The segmented images were then registered to the tissue probability map using affine transformation (i.e., linear, preserving proportions), followed by a nonlinear deformation

in Montreal Institute Neurological (MNI-152) space. The nonlinear deformation parameters were calculated by using the high-dimensional Diffeomorphic Anatomical Registration Through Exponentiated Lie Algebra (DARTEL) algorithm (Ashburner, 2007; Ashburner & Friston, 2009). To correct for expansion (or contraction) during the spatial transformation, the normalized images were then “modulated” by multiplying each voxel by the Jacobian determinant (i.e., linear and nonlinear components) derived from the spatial normalization procedure. Finally, the normalized, modulated gray matter images were then smoothed using an isotropic 5 mm full-width-half-maximum (FWHM) Gaussian filter, and the smoothed images were used for subsequent analysis.

Significant differences in gray matter density were determined in pediatric populations between acute and chronic pain patients under the framework of a general linear model using an independent two-sample *t*-test. To explore gray matter density values in healthy controls, we overlaid the results derived from the between-patients contrasts described above. Here, significant differences between patients (acute and chronic) and healthy controls were then determined using independent two-sample *t*-tests ($p < .05$). In the adult the population, significant differences between chronic pain patients and healthy controls were determined within a general linear model using an independent two-sample *t*-test. For the acute and chronic pediatric comparison, the total intracranial volume and age for each subject were factored out as nuisance variables in the modeling. These parameters were also included as nuisance variables in our adult chronic pain and control comparison. Following an a priori primary threshold of $p < .001$, we applied a family-wise error rate (FWE) cluster-level extent threshold to correct for multiple comparisons. We chose this stringent cluster-defined primary threshold based on the simulations of Woo, Krishnan, and Wager (2014) to optimize the control of false positives and to improve overall inferences about specificity. Significant linear relationships between gray matter density values, pain intensity, and disease duration were determined using Pearson (*r*) correlations.

2.3.2 | Functional connectivity analysis

Using SPM12 (Friston et al., 1994), image preprocessing and seed-based functional connectivity maps were created with the functional connectivity toolbox (Whitfield-Gabrieli & Nieto-Castanon, 2012). Here, prior to realignment, all functional images in pediatric patients with unilateral left pain were flipped to the right (pediatric acute pain, $n = 7$; pediatric chronic pain; $n = 9$).

The first five volumes were then discarded to allow for T1-equilibration effects. All images were subsequently realigned (rigid body translation and rotation) to the first volume as the initial motion correction procedure. The realigned images were then co-registered to the same subjects' T1-weighted anatomical image, and the anatomical images were spatially normalized to MNI-152 space. The deformation field acquired during affine and nonlinear transforms of the T1-weighted anatomical image was then applied to the functional images (i.e., indirect normalization). Finally, the normalized functional images were spatially smoothed with an isotropic 5 mm FWHM Gaussian kernel. Images were linearly detrended to remove global

signal intensity changes and a temporal pass-band filter of 0.01–0.08 Hz applied. To account for nonspecific variance, 18 physiological and motion-related factors were included as nuisance variables, including the first three principle components of the time course derived from separate regions of matter and cerebral spinal fluid (Behzadi, Restom, Liu, & Liu, 2007), and the six body translation and rotation parameters from the realignment procedure. The first temporal derivative of the movement parameters was included to account for temporal shifts in the signal. In recent years, a whole body of literature has established that in-scanner head movement can have substantial influences on resting state functional connectivity (Power, Barnes, Snyder, Schlaggar, & Petersen, 2012; Van Dijk, Sabuncu, & Buckner, 2012), particularly in pediatric populations (Satterthwaite et al., 2012). Here, particular care was taken with examining movement. For all subjects, we set a priori criteria of less than 3 mm cumulative displacement and 3° of angular motion. Three subjects from our sample, made up of two pediatric participants (one chronic, one control) and one adult healthy control, exceeded this criterion and were, therefore, excluded from the functional connectivity analysis.

Using the normalized smoothed images, regions where there were significant contrasts in gray matter density values between the pediatric and adult patients (see above) were used as “seeds” in the subsequent resting state analysis. The seed-based functional connectivity map was generated by computing the correlation coefficient between each voxel's time series with the mean time course of the voxels within the seed region. The individual correlation coefficient maps were then converted to z-maps using Fisher's *r*-to-*z* transformation, and these images were used for group-level statistical comparisons. Given the distribution of scanning parameters, significant group differences between pediatric acute and chronic patients were confined to comparisons with healthy controls that were equally matched to the patient's scanning acquisition. We chose this approach to ensure that any significant group differences were not due to differential scanning parameters (such as repetition time), or influenced by factors such as the degrees of freedom due to differences in the number of volumes acquired. Taken together, significant differences between pediatric acute and chronic pain patients as compared with healthy controls were then determined using an independent two-samples *t*-test, under the framework of a general linear model. Significant differences between adult chronic pain patients and controls were determined under the same framework. For all three comparisons, sex and age were factored out as nuisance variables in the modeling. Significant differences were determined using an a priori primary threshold of $p < .001$ with a family-wise error rate cluster-level extent threshold applied to correct for multiple comparisons. Significant linear relationships between seed-based functional connectivity values, pain intensity, and disease duration were determined using Pearson's correlation analysis ($p < .05$). Finally, to determine whether these significant differences in seed-based connectivity strengths were unique or restricted to a particular pain group, we extracted these regions as a masks, and performed a subsequent region of interest-region of interest functional connectivity analysis across subsequent groups. Significant differences in resting connectivity strengths were then

determined using independent two-sample *t*-tests ($p < .05$). Of course, given the differences in scanning parameters, the purpose of this additional analyses is to provide some indication of specific regional connectivity across all groups, rather than conclusive outcomes, as with the previous analyses.

3 | RESULTS

3.1 | Psychometrics

Individual pediatric (acute and chronic) and adult chronic subject characteristics, imaging modality inclusion, pain duration and pain intensities are shown in Tables 1 and 2, respectively. Our two pediatric groups and one adult group reported, on average, the following: (a) mean [\pm SEM] pain intensity: pediatric acute, 3.97 ± 0.3 ; pediatric chronic, 5.91 ± 0.5 ; adult chronic pain, 4.60 ± 0.5 ; (b) mean [\pm SEM] pain duration (months): pediatric acute, 1.25 ± 0.2 ; pediatric chronic, 15.0 ± 5.4 ; adult chronic pain, 59.67 ± 10.75 ; and (c) pain distribution: pediatric acute, unilateral lower limb extremity, primarily at the distal leg and foot; pediatric chronic, unilateral lower limb extremity, including thigh, leg and foot; adult chronic pain, unilateral upper limb extremity, primarily at distal forearm and hand, with fewer patients reporting pain in the shoulder.

3.2 | Gray matter density

Within the pediatric sample, gray matter density was significantly different between acute and chronic patients in a number of brain regions (Table 3, Figure 1a). Significantly reduced gray matter density values were observed in chronic patients in the left mid-cingulate cortex (mean [\pm SEM] probability*volume; MCC: acute: 0.598 ± 0.023 , chronic: 0.499 ± 0.016 ; $p = .0013$), right inferior temporal gyrus (ITG: acute: 0.576 ± 0.024 , chronic: 0.435 ± 0.018 ; $p = .00007$), right anterior cingulate cortex (ACC: acute: 0.642 ± 0.022 , chronic: 0.543 ± 0.015 ; $p = .0008$), bilaterally in the orbitofrontal cortex (OFC: acute: 0.681 ± 0.019 , chronic: 0.580 ± 0.011 ; $p = .00008$), bilaterally in the thalamic reticular nucleus (TRN: left, acute: 0.173 ± 0.009 , chronic: 0.112 ± 0.005 ; $p = .000002$; right, acute: 0.183 ± 0.012 , chronic: 0.107 ± 0.007 ; $p = .000006$). In contrast, increased gray matter density in chronic patients was observed exclusively within the left ventral posterolateral nucleus of the thalamus (VPL: acute: 0.484 ± 0.019 , chronic: 0.566 ± 0.018 ; $p = .0035$). Furthermore, we report significant linear relationships between these values and pain intensity, as shown in Figure 1b. Positive correlations indicate that greater gray matter density is associated with greater pain intensity occurring in the VPL ($r = .45$, $p = .0098$), whereas a negative relationship was observed within the left and right TRN suggesting less gray matter being associated with greater pain intensity (left: $r = -.48$, $p = .0054$; right: $r = -.36$, $p = .0430$). Furthermore, a negative relationship was observed between pain duration and gray matter density values within the OFC and right TRN (OFC: $r = -.36$, $p = .043$; right TRN: $r = -.35$, $p = .0496$). No other correlations were observed with pain intensity (ITG: $r = -.28$, $p = 0.12$; OFC: $r = -.24$, $p = 0.19$; ACC: $r = -.19$,

TABLE 1 Clinical characteristics of pediatric patients

| Patient (acute) | Pain intensity (0–10) | | Pain duration (months) | | Pain distribution | | Patient (chronic) | Pain intensity (0–10) | | Pain duration (months) | | Pain distribution | | Medication (s) |
|------------------|-----------------------|--------|------------------------|-----------|-------------------|------------------|--------------------|-----------------------|------------|------------------------|------|-------------------|-----------------------------------|----------------|
| | Age | Gender | Age | Gender | Site | Site | | Age | Gender | Site | Site | Medication (s) | | |
| 1 | 19 | M | 3.5 | 0.7 | R | Foot | 17 | F | 7.0 | 3 | R | Leg, foot | Gabapentin | |
| 2 | 19 | F | 2.0 | 0.6 | R | Foot | 18 | M | 3.0 | 8 | L | Leg, foot | Gabapentin, citalopram, clonidine | |
| 3 | 17 | F | 4.0 | 1.9 | R | Foot | 19 ^b | M | 7.0 | 12 | R | Knee, foot | Amitriptyline | |
| 4 | 15 | F | 3.5 | 0.7 | L | Distal leg, foot | 20 | F | 2.5 | 48 | L | Leg, foot | Doxepin | |
| 5 | 12 | F | 4.0 | 0.8 | L | Foot | 21 | F | 6.0 | 19 | L | Leg, foot | Pregabalin | |
| 6 | 18 | M | 5.0 | 0.9 | R | Foot | 22 | F | 7.5 | 3 | L | Leg, foot | Duloxetine | |
| 7 | 22 | M | 4.5 | 0.6 | L | Foot | 23 | F | 6.0 | 85 | R | Leg, foot | Gabapentin | |
| 8 ^a | 15 | M | 6.0 | 1.7 | L | Foot | 24 | F | 5.5 | 13 | L | Leg, foot | Amitriptyline | |
| 9 | 14 | M | 4.5 | 1.5 | L | Foot | 25 | M | 7.0 | 5 | R | Leg, foot | Gabapentin | |
| 10 | 15 | F | 4.0 | 1.4 | R | Foot | 26 | M | 4.0 | 11 | L | Knee | - | |
| 11 | 16 | F | 2.5 | 1.1 | R | Foot | 27 | F | 3.5 | 3 | R | Thigh, leg, foot | - | |
| 12 | 15 | M | 5.5 | 1.0 | L | Foot | 28 | F | 8.0 | 9 | L | Leg, foot | - | |
| 13 | 15 | F | 4.5 | 0.9 | R | Foot | 29 | F | 7.0 | 10 | R | Leg, foot | Gabapentin | |
| 14 | 12 | F | 4.5 | 0.9 | L | Foot | 30 | M | 6.0 | 3 | L | Leg, foot | - | |
| 15 | 13 | F | 3.0 | 3.1 | R | Distal leg, foot | 31 | M | 7.0 | 3 | R | Leg, foot | - | |
| 16 | 16 | F | 2.5 | 2.1 | R | Foot | 32 | F | 5.5 | 6 | L | Foot | Gabapentin, ibuprofen, Doxepin | |
| Acute mean ± SEM | 15.8 ± 0.6 | | 3.97 ± 0.3 | 1.2 ± 0.2 | | | Chronic mean ± SEM | 14.3 ± 0.6 | 5.91 ± 0.5 | 15.0 ± 5.4 | | | | |

Abbreviations: F, female; L, left; M, male; R, right.

^aRemoved from seed-based connectivity analysis due to failed image acquisition.

^bRemoved from seed-based connectivity analysis due to excessive head motion. Note that brain images for all patients with unilateral left pain were flipped to the right.

TABLE 2 Clinical characteristics of adult patients

| Patient (chronic) | Age | Gender | Pain intensity (0–10) | Pain duration (months) | Site | Pain distribution | Medication(s) |
|-------------------|----------|--------|-----------------------|------------------------|------|--------------------|--|
| 1 | 54 | F | 1 | 11 | R | Distal hand | Metamizole, tramadol, gabapentin |
| 2 | 67 | F | 5 | 140 | R | Hand, forearm | - |
| 3 | 56 | M | 4 | 64 | R | Arm, forearm, hand | Metamizole, pregabalin |
| 4 | 67 | M | 4 | 77 | R | Distal hand | - |
| 5 | 59 | M | 4 | 50 | R | Distal hand | - |
| 6 | 71 | F | 4 | 126 | R | Distal hand | Aspirin, metamizole, tramadol |
| 7 | 46 | F | 2 | 80 | R | Distal hand | Metamizole |
| 8 | 62 | F | 8 | 7 | R | Arm, forearm, hand | Metamizole, tramadol |
| 9 | 69 | F | 6 | 144 | R | Distal hand | Ibuprofen, aspirin |
| 10 | 37 | F | 3 | 103 | R | Distal hand | Ibuprofen, metamizole |
| 11 | 47 | F | 8 | 57 | R | Arm, forearm, hand | Oxycodone |
| 12 | 55 | M | 6 | 109 | R | Arm, forearm, hand | Ibuprofen, metamizole |
| 13 | 67 | F | 2 | 105 | R | Distal hand | Ibuprofen, pregabalin |
| 14 | 58 | F | 5 | 15 | R | Hand, forearm | - |
| 15 | 57 | F | 3 | 8 | R | Distal hand | - |
| 16 | 66 | F | 4 | 6 | R | Distal hand | Metamizole, tilidine, amitriptyline |
| 17 | 53 | F | 9 | 39 | R | Distal hand | - |
| 18 | 53 | M | 6 | 19 | R | Arm, forearm, hand | Ibuprofen, metamizole |
| 19 | 64 | F | 1 | 19 | R | Distal hand | - |
| 20 | 51 | M | 7 | 13 | R | Hand, forearm | Metamizole, tilidine, gabapentin, duloxetine |
| Mean ± SEM | 57.9 ± 9 | | 4.60 ± 0.5 | 59.7 ± 10.8 | | | |

Abbreviations: F, female; M, male; R, right.

$p = .30$; MCC: $r = -.08$, $p = .66$) or disease duration (ITG: $r = -.10$, $p = .59$; ACC: $r = -.31$, $p = .08$; MCC: $r = -.26$, $p = .15$; VPL: $r = .16$, $p = .38$; left TRN: $r = -.28$, $p = .12$). In summary, compared with pediatric acute pain patients, pediatric chronic pain patients were associated with widespread reduced gray matter density within sensory (VPL)-emotional (MCC, ACC)-descending (OFC) regions, as compared with an increase in sensory modulatory (TRN) region, whereby significant correlations were confined within somatosensory related processing and modulation (VPL and TRN).

Gray matter density values were then extracted in pediatric healthy controls from significant clusters derived from the previous acute and chronic analysis described above. Compared with healthy controls, significant differences in acute and chronic patients were observed in a number of brain regions (Figure 2). Here, compared with acute patients, healthy controls displayed reduced gray matter density within the ITG (mean [\pm SEM] probability*volume; controls: 0.493 ± 0.017 ; two sample t -test, $p = .007$) and OFC (controls: 0.635 ± 0.010 , $p = 0.024$). No other differences were observed as compared with the acute patient group (ACC: controls: 0.652 ± 0.017 , $p = .75$; MCC: controls: 0.550 ± 0.013 , $p = .051$; VPL: controls: 0.504 ± 0.014 , $p = .42$; left TRN: controls: 0.148 ± 0.009 , $p = .097$; right TRN: controls: 0.162 ± 0.010 , $p = .23$). In contrast, significant differences were observed in all regions when comparing healthy controls with chronic

pain patients. Specifically, chronic pain patients displayed reduced gray matter density within the ITG (two sample t -test, $p = .043$), OFC ($p = .0014$), ACC ($p = .0002$), MCC ($p = .023$), left TRN ($p = .011$) and the right TRN ($p = .0008$), as compared with controls. Conversely, compared with controls, chronic pain patients were associated with increased gray matter density within the VPL ($p = .012$).

Within the adult sample, gray matter density differed significantly between chronic patients and healthy controls in sensory and emotional-related brain sites (Table 4, Figure 3a). Specifically, chronic pain patients displayed significantly reduced gray matter density within the left VPL (mean [\pm SEM] probability*volume; chronic: 0.506 ± 0.014 , controls: 0.593 ± 0.015 ; $p = .00016$), whereas an increase was observed in the left ACC (chronic: 0.354 ± 0.001 , controls: 0.328 ± 0.01 ; $p = .0085$). Finally, no significant correlations were observed between these values and pain intensity (VPL: $r = .02$, $p = .93$; ACC: $r = -.33$, $p = .16$) and disease duration (VPL: $r = -.03$, $p = .33$; ACC: $r = .13$, $p = .59$; Figure 3b).

3.3 | Resting functional connectivity

Using the clusters derived from the gray matter density analysis as "seeds," resting functional connectivity strengths were determined to be significantly different in a number of brain sites across pediatric and adult groups (Table 5, Figure 4). Specifically, in pediatric acute patients,

TABLE 3 Regions in which gray matter density was significantly different in acute compared with chronic pediatric patients

| | X | Y | Z | t-statistic value | Cluster size | p-value |
|-------------------------------------|-----|-----|-----|-------------------|--------------|---------|
| <i>Acute > chronic</i> | | | | | | |
| Left thalamic reticular nucleus | -25 | -20 | 16 | 8.42 | | |
| | -26 | -19 | 11 | 6.81 | 434 | .047 |
| | -22 | -14 | 11 | 6.22 | | |
| Left mid-cingulate cortex | -6 | 14 | 33 | 5.01 | | |
| | -7 | 9 | 35 | 4.72 | 930 | .001 |
| | -7 | 17 | 30 | 4.62 | | |
| Right thalamic reticular nucleus | 25 | -19 | 17 | 6.65 | 483 | .028 |
| | 22 | -17 | -4 | 6.39 | | |
| Right inferior temporal gyrus | 55 | -30 | -27 | 4.97 | | |
| | 48 | -23 | -32 | 4.70 | 564 | .013 |
| | 61 | -35 | -28 | 4.24 | | |
| Right anterior cingulate nucleus | 11 | 32 | 22 | 6.45 | | |
| | 9 | 42 | 23 | 5.60 | 942 | .0001 |
| | 16 | 36 | 22 | 4.45 | | |
| Bilateral orbitofrontal cortex | -25 | 5 | -18 | 9.13 | | |
| | 3 | 17 | -23 | 7.92 | 6,638 | .0001 |
| | -4 | 18 | -23 | 7.42 | | |
| <i>Acute < chronic</i> | | | | | | |
| Left ventral posterolateral nucleus | -19 | -25 | 5 | 5.08 | 503 | .046 |

Locations are in Montreal Neurological Institute space. Significant clusters were from cluster-extent thresholding (family-wise error rate) to correct for multiple comparisons.

significantly greater OFC resting connectivity strength occurred in the right hippocampus (mean [\pm SEM] parameter estimate values; pediatric acute: 0.35 ± 0.02 , controls: 0.09 ± 0.05 ; two-sample *t*-test, $p = .00002$), as compared with healthy controls (Figure 4a). In contrast, pediatric chronic patients had significantly reduced VPL resting connectivity strengths with the left and right primary somatosensory cortex (SI: pediatric chronic: -0.07 ± 0.02 , controls: 0.13 ± 0.02 ; $p = .000001$) (Figure 4b). Compared with controls, adult chronic pain patients exhibited significantly greater ACC connectivity strength with SI (adult chronic pain: 0.08 ± 0.03 , controls: -0.08 ± 0.02 ; $p = .00002$) and reduced VPL connectivity with the posterior cingulate cortex (PCC: adult chronic pain: -0.03 ± 0.03 , controls: 0.15 ± 0.03 ; $p = .00009$; Figure 4C). Extraction of these resting functional connectivity values revealed no significant correlations with pain intensity (OFC-HPC: $r = -.30$, $p = .28$; VPL-SI: $r = -.45$, $p = .09$; ACC-SI: $r = -.04$, $p = .87$; VPL-PCC: $r = -.32$, $p = .17$) or disease duration (OFC-HPC: $r = -.49$, $p = .064$; VPL-SI: $r = .29$, $p = .29$; ACC-SI: $r = .36$, $p = .12$; VPL-PCC: $r = -.05$, $p = .83$). Using the clusters derived from the seed-based functional connectivity strengths, we performed a region of interest-region of interest functional connectivity analysis across all groups and their respective controls. Here, no significant differences were observed across the groups, that is, these significant seed-based functional strengths were restricted to each group in pediatric acute OFC-HPC (pediatric chronic: 0.14 ± 0.04 , controls: 0.13 ± 0.05 ; two-sample *t*-test, $p = .88$; adult chronic pain: 0.11 ± 0.04 , controls: 0.10 ± 0.04 ; $p = .87$), pediatric chronic VPL-SI (pediatric acute: 0.07 ± 0.04 , controls: 0.08 ± 0.04 ; two-sample *t*-test, $p = .95$; adult chronic pain: 0.14 ± 0.04 ,

controls: 0.13 ± 0.04 ; $p = .81$) and adult chronic pain ACC-SI (pediatric acute: 0.01 ± 0.05 , controls: -0.10 ± 0.12 ; two-sample *t*-test, $p = .12$; pediatric chronic: -0.04 ± 0.04 , controls: -0.03 ± 0.05 ; $p = .88$) and VPL-PCC (pediatric acute: 0.15 ± 0.04 , controls: 0.10 ± 0.03 ; two-sample *t*-test, $p = .34$; pediatric chronic: 0.12 ± 0.04 , controls: 0.06 ± 0.04 ; $p = .33$). In summary, compared with controls: (a) pediatric acute pain patients had greater functional connectivity strengths between the OFC and the HPC; (b) pediatric chronic patients had greater functional connectivity strengths between the VPL and MI-SI; (c) adult chronic patients had greater functional connectivity strengths between the ACC and SI, whereas the VPL had reduced connectivity with the PCC; (d) In all these groups, no significant correlations were observed between functional connectivity strengths and pain intensity or disease duration.

3.4 | Somatotopic representation of upper and lower limb

In this investigation, we report structural and functional alterations in brain sites of pediatric and adult chronic pain patients with a somatotopic representation, notably the thalamus and primary somatosensory cortex (Figure 5). Specifically, we report altered gray matter density in the ventral posterolateral nucleus of the thalamus that is consistent with upper and lower limb somatotopy, that is, lateral to medial, respectively (Kaas et al., 1984). Moreover, we report altered resting functional connectivity with the primary

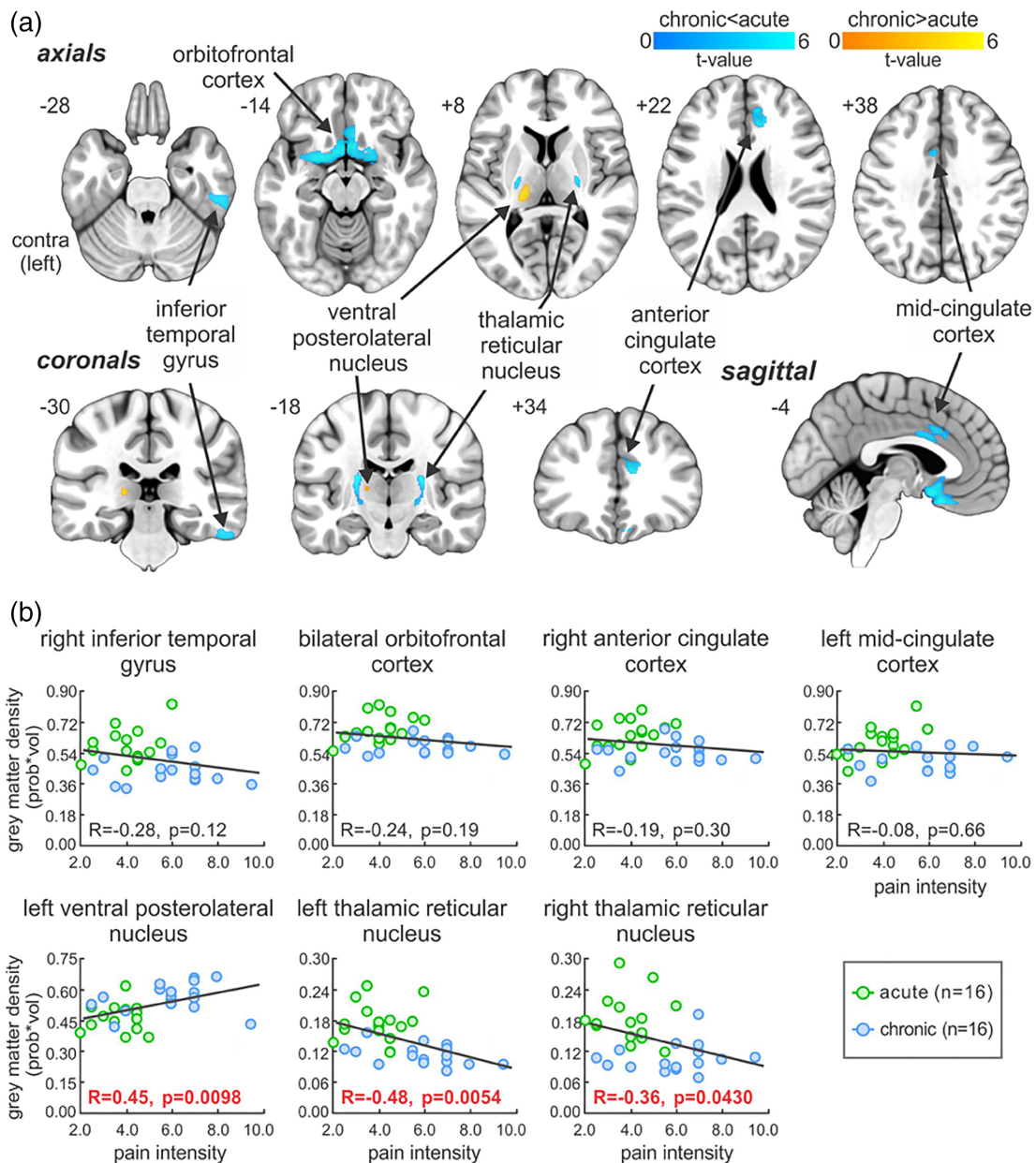


FIGURE 1 Whole brain gray matter density analysis between pediatric chronic versus acute. (a) Brain sites in which significantly reduced (cool color scale) or increased (warm color scale) gray matter density was observed in pediatric chronic pain as compared with patients with acute pain, overlaid onto axial, coronal and sagittal T1-weighted anatomical image set. Slice locations are located on the top left of each image and are in Montreal Neurological Institute space. (b) Correlation between regional gray matter density values within these regions against pain intensity. Note that significant correlations were confined to brain sites associated with somatosensory related processing and modulation, that is, the ventral posterolateral nucleus of the thalamus and the thalamic reticular nucleus [Color figure can be viewed at wileyonlinelibrary.com]

somatosensory cortex, consistent with upper limb (anterolateral) and lower limb (posteromedial) somatotopy (Penfield & Boldrey, 1937).

4 | DISCUSSION

The underlying pathophysiology of the evolution of acute to chronic pain remains unknown. Here we used an approach to evaluate two concepts: (a) is there a difference in brain systems in acute and chronic pain affecting the same region of the body? and (b) is there a difference in the same

disease affecting the brain in pediatric vs. adult onset CRPS? In both cases we focused on somatosensory systems for the following reasons: (a) they are well defined and have a known physiology in pain; (b) somatotopy can be relatively easily defined with current imaging technology; (c) comparisons between pediatric and adult region specific areas can be evaluated; (d) these areas are less likely to be influenced by comorbid processes, such as anxiety and depression. Our primary results indicate that there is a shift in gray matter density alterations from pediatric acute (descending modulatory) to pediatric chronic (descending modulatory/sensory-affective) to adult chronic pain (sensory-affective)

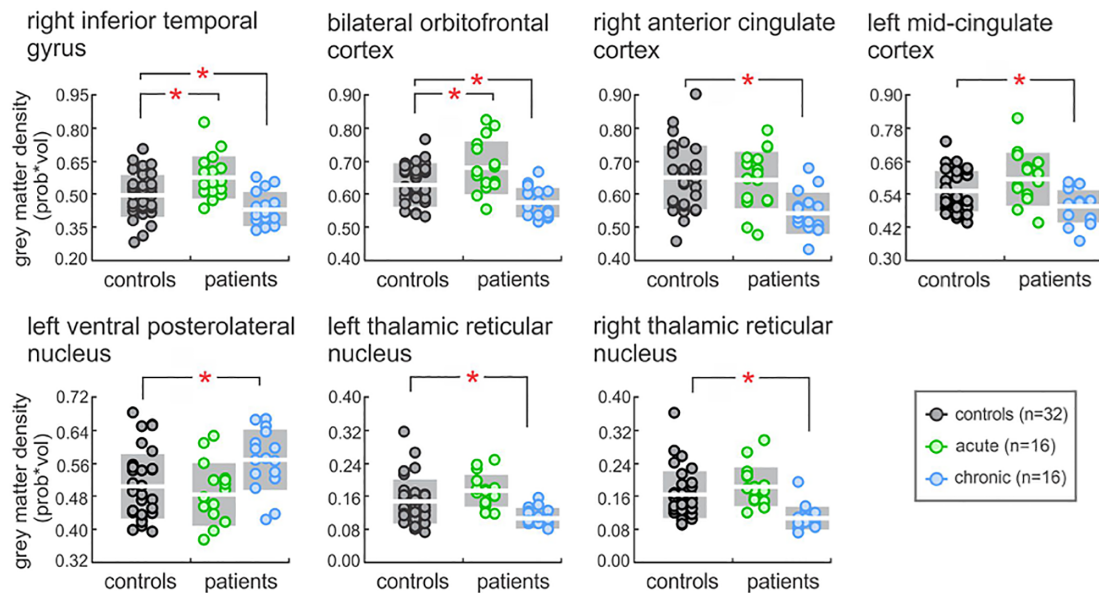


FIGURE 2 Plots of gray matter density values in patients (acute and chronic) and healthy controls. Note that these values were derived from overlaying significant clusters from the patient contrast previously described. Significant between-group differences were determined using independent two-sample *t*-test ($*p < .05$). Note that the white horizontal line reflects the mean, whereas gray shading represents one standard deviation above and below, within each group [Color figure can be viewed at wileyonlinelibrary.com]

TABLE 4 Regions in which gray matter density was significantly different in adult chronic patients as compared with healthy controls

| | X | Y | Z | t-statistic value | Cluster size | p-value |
|-------------------------------------|-----|-----|----|-------------------|--------------|---------|
| <i>Chronic > controls</i> | | | | | | |
| Left anterior cingulate cortex | -14 | 15 | 34 | 5.44 | | |
| | -9 | 17 | 39 | 5.33 | 1,215 | .046 |
| | -14 | 19 | 35 | 5.15 | | |
| <i>Chronic < controls</i> | | | | | | |
| Left ventral posterolateral nucleus | -12 | -17 | 2 | 4.66 | 1,220 | .045 |
| | -8 | -5 | 8 | 3.65 | | |

Note: Locations are in Montreal Neurological Institute space. Significant clusters were from cluster-extent thresholding (family-wise error rate) to correct for multiple comparisons.

across brain sites. In addition, patterns of resting functional connectivity strengths were distinctive across pain conditions and age groups; notably, strengths progressed from descending modulatory memory-related circuits in acute pain to sensory-sensory changes in pediatric chronic to sensory-affective alterations in adult chronic pain. However, it is pertinent to note that we do not argue specific systems (e.g., descending modulatory) exclusively, and instead provide a framework that may correspond to a shift in brain sites from pediatric acute and chronic pain to adult chronic pain. Finally, an overlay of these differences in pediatric (lower limb) and adult (upper limb) chronic pain within VPL and SI revealed differential patterns of structural and functional metrics that were consistent with well-established somatotopical arrangements.

4.1 | Similarities and differences in pediatric and adult CRPS brain

Of the few studies that have explored structural brain metrics in CRPS, a common trend of gray matter atrophy is evident across

pediatric and adult populations. Interestingly, compared with controls, comparison with our previous investigation (Erpelding et al., 2016) and others, reveal widespread (sensory, motor, emotional, cognitive, descending modulatory-related) brain alterations in pediatric CRPS (Erpelding et al., 2016), whereas adult CRPS report fewer alterations across sensory, emotional, and descending modulatory-related brain sites (Baliki, Schnitzer, Bauer, & Apkarian, 2011; Barad et al., 2014; Geha et al., 2008). In the present study, we report a similar trend, with sensory (VPL)-emotional (MCC, ACC)-descending (OFC) and sensory modulatory (TRN) alterations in pediatric CRPS, whereas a shift to sensory (VPL)-emotional (ACC) changes in adult CRPS. Finally, it is pertinent to note that although these differences in pediatric CRPS were present when compared with controls, comparison was restricted to those regions that were derived from comparing with acute subjects. This is an important consideration since, it is well established that a number of brain sites are engaged during acute pain perception (Farrell, Laird, & Egan, 2005; Henderson, Bandler, Gandevia, & Macefield, 2006). In any case, comparison within the

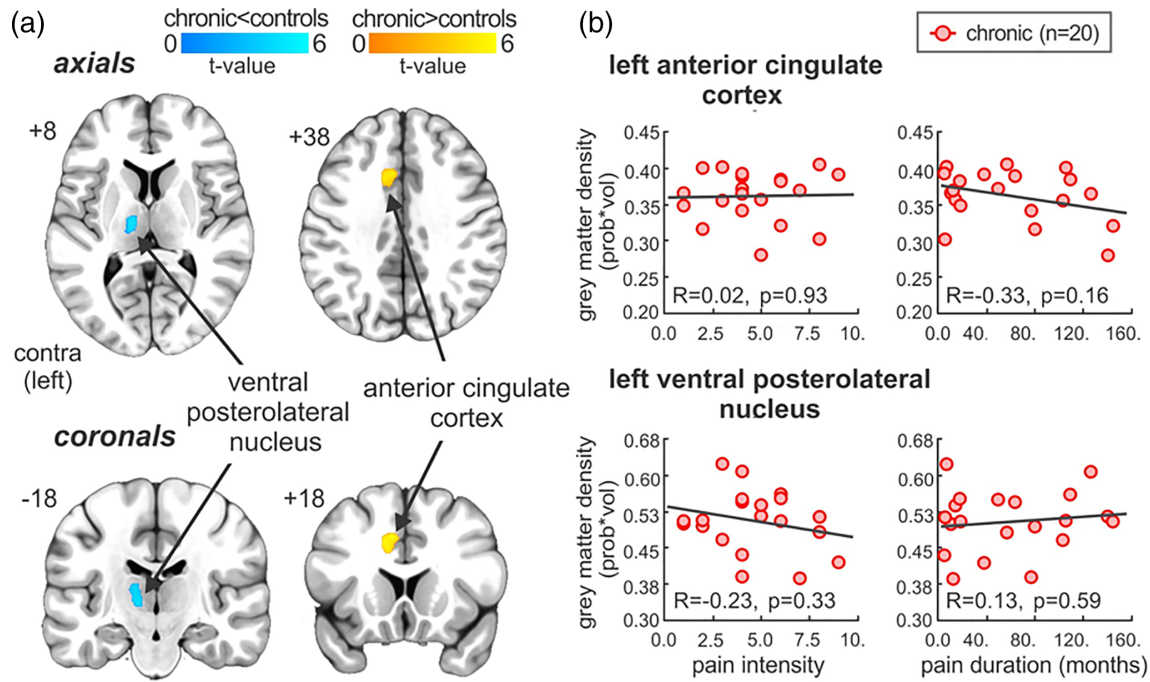


FIGURE 3 Whole brain gray matter density analysis between adult chronic and healthy controls. (a) Regional gray matter density reduced within the ventral posterolateral thalamic nucleus (cool color bar) and increased within the anterior cingulate cortex (warm color bar) in adult chronic as compared with controls, overlaid onto an axial and coronal T1-weighted anatomical image set. Slice locations are located on the top left of each image and are in Montreal neurological institute space. (b) Correlations between regional gray matter density values within these regions against pain intensity and disease duration. Note that no significant correlations were observed [Color figure can be viewed at wileyonlinelibrary.com]

TABLE 5 Regions in which seed-based resting functional connectivity strengths were significantly different across pediatric (acute and chronic) and adult (chronic) groups, as compared with healthy controls

| | X | Y | Z | t-statistic value | Cluster size | p-value |
|---|-----|-----|-----|-------------------|--------------|---------|
| <i>Pediatric acute > controls</i> | | | | | | |
| Orbitofrontal cortex "seed" | | | | | | |
| Right hippocampus | 28 | -28 | -16 | 4.84 | | |
| | 24 | -26 | -16 | 4.80 | 152 | .013 |
| | 16 | -32 | -20 | 3.95 | | |
| <i>Pediatric chronic < controls</i> | | | | | | |
| Ventral posterolateral nucleus "seed" | | | | | | |
| Bilateral primary motor cortex/primary somatosensory cortex | 2 | -18 | 60 | 6.39 | | |
| | 0 | -32 | 62 | 4.74 | 254 | .0001 |
| | -4 | -22 | 68 | 3.93 | | |
| <i>Adult chronic > controls</i> | | | | | | |
| Anterior cingulate cortex "seed" | | | | | | |
| Left primary somatosensory cortex | -50 | -24 | 62 | 5.46 | | |
| | -36 | -26 | 66 | 4.61 | 93 | .048 |
| | -34 | -30 | 62 | 4.38 | | |
| <i>Adult chronic < controls</i> | | | | | | |
| Ventral posterolateral nucleus "seed" | | | | | | |
| Bilateral posterior cingulate cortex | -2 | -30 | 44 | 4.30 | | |
| | 0 | -24 | 38 | 4.00 | 137 | .023 |
| | 6 | -14 | 34 | 3.75 | | |

Note: "seed" clusters were derived from the previous pediatric and adult gray matter density analyses. Locations are in Montreal Neurological Institute space. Significant clusters were from cluster-extent thresholding (family-wise error rate) to correct for multiple comparisons.

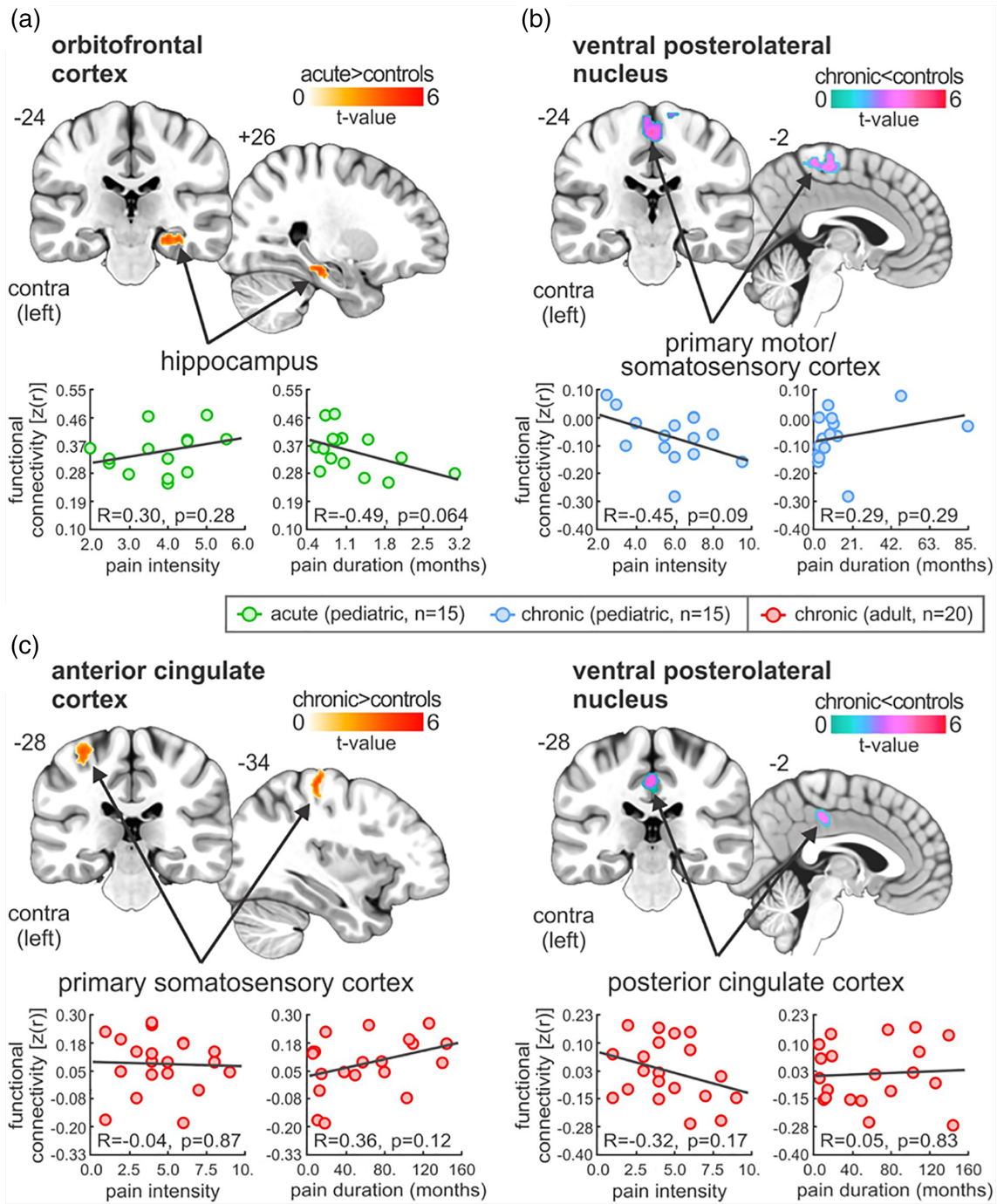


FIGURE 4 Significant differences in seed-based functional connectivity in pediatric (acute and chronic) and adult chronic as compared with controls. (a) Plots of resting seed-based functional connectivity from orbitofrontal cortex cluster, derived from pediatric acute and chronic gray matter density analysis. Note that compared with controls, acute patients have significantly greater functional connectivity strengths between the orbitofrontal cortex and the hippocampus. (b) Plots of resting seed-based functional connectivity from ventral posterolateral thalamic nucleus cluster, derived from pediatric chronic and healthy control gray matter density analysis. Note that compared with controls, pediatric chronic patients have significantly greater functional connectivity strengths between the ventral posterolateral thalamic nucleus and the primary motor and somatosensory cortex. (c) Plots of resting seed-based functional connectivity from anterior cingulate cortex and ventral posterolateral thalamic nucleus clusters, derived from between adult chronic and healthy control gray matter density analysis. Note that compared with controls, adult chronic patients have significantly greater functional connectivity strengths between the anterior cingulate cortex and the primary somatosensory cortex, whereas ventral posterolateral thalamic nucleus had reduced connectivity with the posterior cingulate cortex. Note that no significant correlations were observed between these values and pain intensity or disease duration ($p > .05$) [Color figure can be viewed at wileyonlinelibrary.com]

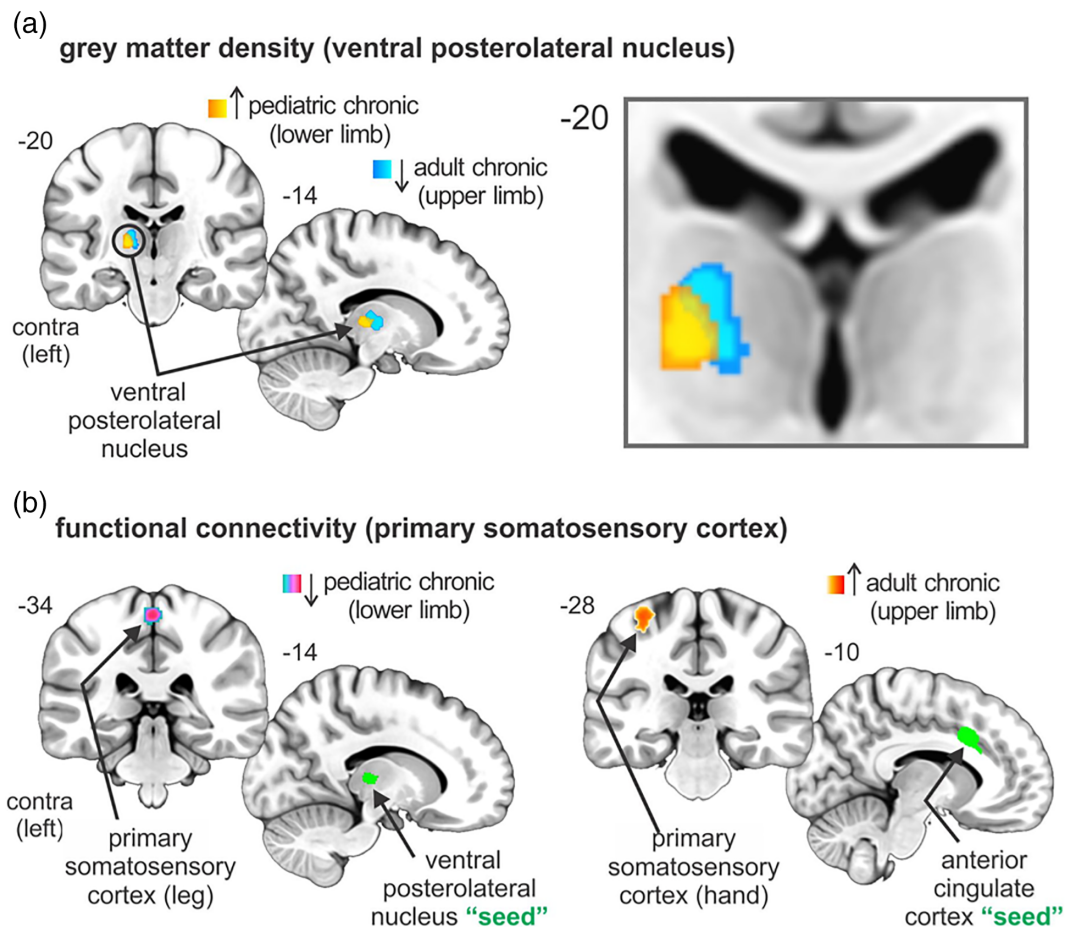


FIGURE 5 Overlay of significant pediatric and adult chronic structural and functional clusters within the ventral posterolateral thalamic nucleus and the primary somatosensory cortex. (a) Altered gray matter density in the ventral posterolateral nucleus of the thalamus that are consistent with upper (adult) and lower (pediatric) limb somatotopy, that is, lateral to medial, respectively. Note that increased gray matter density in pediatric chronic patients was reported relative to both pediatric acute patients and healthy controls. (b) Altered resting functional connectivity strengths within the primary somatosensory cortex, consistent upper limb (anterolateral) and lower limb (posteromedial) somatotopic organization [Color figure can be viewed at wileyonlinelibrary.com]

same brain site in pediatric and adult CRPS revealed a differential pattern of gray matter density alterations in sensory (VPL) and emotional (ACC)-related brain regions.

In addition to structural metrics, differential resting functional connectivity patterns have been reported across age groups. Here, our previous functional brain imaging investigations have revealed widespread hyperconnectivity patterns, notably within fear-related (Simons et al., 2014), pain modulatory circuits (Erpelding et al., 2016), and the default mode network (Becerra et al., 2014), among others. Comparably, in adult CRPS, the inverse pattern of covariation is observed, notably widespread hypoconnectivity patterns have been shown within sensory and affective brain regions (Kim, Choi, et al., 2017) and within the default mode network (Bolwerk et al., 2013). Interestingly, Kim, Choi, et al. (2017) reported altered SI covariation with both affective (anterior insula) and sensory (posterior insula) processing. In our investigation, we report the inverse pattern of connectivity with SI, that is, hyperconnectivity with an affective-motivational (ACC) brain site. Although possible, this is not to suggest that the ACC has a direct integrative role on SI somatotopic

processing, since while the VP-SI circuitry is well established, the role of the SI-ACC integration remains relatively unclear. Instead, it is possible that the ACC may integrate SI processing indirectly through VP or TRN alteration, and a lack of observed difference in this study may correspond due to technical limitations such as relatively increased voxel size and smoothing kernel. In any case, it is pertinent to note that in this study patterns of resting functional connectivity were distinctive across pain conditions and age groups. Compared with controls, we report altered resting functional connectivity strengths between descending modulatory (OFC) and memory-related (hippocampus) brain sites in acute pain, within sensory (VPL-SI) regions in pediatric chronic pain, and between sensory-affective (ACC-SI) and sensory-working memory/awareness (VPL-PCC) in adult chronic pain.

4.2 | Somatotopic representation of lower (pediatric) and upper (adult) limb: Fidelity of approach

As noted in the introduction, we utilized the somatotopic organization of the afferent somatosensory pain system to define changes within

the three patient groups and their matched controls. The approach provides a clear fidelity to the data presented. Thalamic somatotopy for pain pathways has been described in rodents (Willis, 1985), non-human primates (Kaas et al., 1984; Ralston 3rd., 2005) and humans (Lenz et al., 1988). SI is one of the most investigated and well-described human brain regions. It encompasses the postcentral gyrus on both the left and right sides of the brain and has a well described somatotopic map, with the leg represented medially in the paracentral lobule and the hand and face more laterally towards the parietal operculum. A few fMRI studies have examined somatotopy of the somatosensory pathway in healthy subjects (DaSilva et al., 2002; Hong, Kwon, & Jang, 2011) and in pain patients (Maleki et al., 2012; Shokouhi et al., 2017) and their connectivity (Yamada et al., 2007). Both these regions show plasticity in pain (Hubbard et al., 2016; Kim, Kim, et al., 2017). Here we report altered gray matter density in the VPL thalamus that is consistent with upper and lower limb somatotopy, that is, lateral to medial, respectively (Kaas et al., 1984).

4.3 | Gray matter changes follow somatotopic organization

In patients with CRPS affecting the foot (pediatric group) and hand (adult group), changes in gray matter show a high degree of somatotopic organization within the somatosensory thalamus (VPL) and somatosensory cortex (SI). Changes in the organization of the ventroposterior lateral thalamus have been reported with sensory deprivation that may induce reorganization in SI (Rasmusson, 1996) with subsequent changes in function. Changes in gray matter volume within the thalamus have been reported in humans with chronic pain (Lutz et al., 2008), but few imaging studies have focused on specificity of somatotopy in chronic pain. Clearly, the thalamus offers an opportunity to define changes in pain within regions that have clearly defined somatotopy. Furthermore, changes within these regions may provide insights into hypersensitivity (Nagasaka, Takashima, Matsuda, & Higo, 2017). The changes have secondary effects on brain connectivity since these areas connect with other brain regions including well-defined areas such as SI and those that are not well recognized, such as the substantia nigra, VPL (Antal, Beneduce, & Regehr, 2014) and superior temporal sulcus (Yeterian & Pandya, 1989). Here, we are the first to report somatotopic alterations within the somatosensory thalamus. It is pertinent to note that thalamic reduction in gray matter density has been reported across a range of chronic pain syndromes (Apkarian et al., 2004). In fact, in neuropathic pain syndromes, decreased blood flow is often exclusively reported in the thalamus (Moisset & Bouhassira, 2007). Furthermore, we report an increase in gray matter density within the ACC, perhaps reflecting increased dominance of the affective-motivational role in our adult population. Specific evaluation of brain regions involved in affective-motivational processing was not the focus of this study. Moreover, it may reflect age-related differences, since our adult population is, on average, 10 years older than previous studies.

4.4 | Acute versus chronic pain in the pediatric brain: Potential insights into somatosensory chronification

Comparison of structural and functional metrics revealed distinct alterations in sensory-discriminative regions with a well-described somatotopic organization (VPL, SI). Moreover, we report alterations within the TRN, a region heavily associated with collateral and terminal branches of the VPL thalamocortical projection neurons, which send collaterals to the TRN and which itself contains GABAergic neurons which project to the VPL thalamus (Lam & Sherman, 2011). As a result, altered VPL-SI, SI-VPL, and TRN-VPL circuitry may result in a disturbance of the normal patterning of activity within the cortex, which may result in the constant perception of pain. Indeed, recent investigations have demonstrated that changes in thalamic function may result in widespread whole brain activity changes and that chronic pain may arise as a consequence of thalamocortical dysrhythmia (Alshelh et al., 2016; Walton, Dubois, & Llinas, 2010). In support, these thalamocortical loops have been shown to involve collaterals to GABAergic neurons in the TRN (Pinault, 2004), and remarkably, investigations have shown reduced thalamic blood flow gray matter density, neural viability and GABAergic content (Gustin et al., 2011; Youssef et al., 2014) and, specifically within the TRN, reduced blood flow and increased infra-slow oscillation power and network connectivity in patients with neuropathic pain (Alshelh et al., 2016; Gustin et al., 2014; Henderson et al., 2013). The reports, in conjunction with our findings, support the idea above, that although there is no obvious nerve injury in Type I patients, one cannot exclude the possibility of a subtle nerve injury that propagates along the ascending tract. Compared with acute, we found gray matter increased within the contralateral (left) VPL in pediatric chronic patients, whereas atrophy was reported bilaterally within the TRN. Furthermore, in this study, we found an association between pain intensity and gray matter density that were exclusive with these somatosensory-related regions, notably within the contralateral VPL and bilateral TRN. Although we did not observe any alterations within SI, it is pertinent to note that given the widespread somatotopic organization, it is possible that a lack of SI alteration may reflect the nature of the group analyses, that is, the fine somatotopic representation of SI between individual subjects may result in no overall SI group difference. Alternatively, it may be that acute subjects are associated with SI gray matter atrophy, or no change, corresponding with pediatric CRPS.

In addition, we reveal differential alterations in resting functional connectivity patterns in the pediatric acute (ankle sprain) versus chronic (CRPS) patients compared with controls. Specifically, pediatric acute had greater rFC strength between the OFC and the hippocampus. In contrast, pediatric CRPS had altered sensory circuit connectivity, that is, reduced rFC between the VPL and SI. Given these differences, the acute stage appears to reflect alterations in pain modulatory and memory-related circuitry, whereas a shift to sensory-circuits appears during the chronic phase. The latter is counter to prior work showing a shift of acute pain from sensory to emotional circuits, previously reported in the adult back pain patients (Hashmi et al., 2013). The shift in rFC from acute to chronic pain in pediatric

populations highlights a trend from initial pain modulatory distribution in acute to sensory-affective circuits in chronic pain. Furthermore, we report an age-related shift in chronic pain, with a sensory-emotional alteration in our adult populations, a finding that is consistent with pain chronification in adults (Hashmi et al., 2013). Indeed, given the age-related shift across the same chronic pain syndrome, our results may contribute to the well-known differences between child and adult pain vulnerability and resilience.

5 | LIMITATIONS

We note the following limitations of this study: (a) *Sex*: Given that our cohort was predominantly female, we did not have the statistical power to explore sex-related differences. We cannot exclude the possibility that some of the observed changes may be related to hormonal/menstrual changes in our subjects; (b) *CRPS subtype*: We did not specify the subtype of CRPS but grouped the patients. Clinically, patients had signs and symptoms of neuropathic involvement. If measures of nerve fiber integrity and function could have been used (including single fiber microneurography), alterations in fiber function could be more fully defined. Thus, is thus a difficult issue to define since while obvious nerve injury is observed in some cases it is not clearly defined in Type 1 CRPS. (c) *Pain intensity and duration*: For the acute and chronic pediatric comparison, the total pain intensity and duration differed between the groups, and therefore our results may, in part, be influenced by baseline differences in these parameters; (d) *Technical*: Given that we used different scanning parameters for group comparisons, particularly in the functional connectivity analyses, it is pertinent to note that for each contrast, group differences were relative to control groups that were sequence matched. Despite this, we acknowledge that we cannot completely exclude influences of parameter factors such as repetition time (signal covariation timeframe) and volume series (influence of degrees of freedom) on the observed results; (e) *Image flip*: Given that we flipped the patients' brain, for those with unilateral left-sided pain, it is pertinent to mention that this may reflect laterality in brain networks (Kucyi, Hodaie, & Davis, 2012; Vukelic et al., 2014). However, given the relatively small sample size of our pediatric patients, and the focus on somatosensory systems, we believe this approach is most appropriate; and (f) *Age and brain development*: we are aware that differential trajectories in gray matter density (Bourisly et al., 2015; Gennatas et al., 2017) and functional connectivity strengths (Chou, Chen, & Madden, 2013; Grady, Sarraf, Saverino, & Campbell, 2016) patterns across brain regions and networks may differ, and that inclusion of age does not completely mitigate this influence.

6 | CONCLUSIONS

These data reveal shift in gray matter density alterations from pediatric acute (descending modulatory) to pediatric chronic (descending modulatory/sensory-affective) to adult chronic pain (sensory-affective) across brain sites. Furthermore, our data reveals a shift in resting functional connectivity circuits, from sensory alterations in pediatric

populations to sensory-emotional alterations in adult populations that are consistent with well-established somatotopical arrangements.

ACKNOWLEDGMENTS

Research reported in this study was supported by NIH grants (R01NS065051; K24NS064050 to DB and K23HD067202 to LS) and the MayDay Fund, New York (DB). The content is solely the responsibility of the authors and does not necessarily represent the official views of the National Institutes of Health or the Mayday Fund.

CONFLICT OF INTERESTS

The authors declare that they have no competing interests. DB Consults to Biogen unrelated to the material in this manuscript.

ORCID

Andrew M. Youssef  <https://orcid.org/0000-0001-8025-3080>

David Borsook  <https://orcid.org/0000-0001-9825-0064>

REFERENCES

- Alshelhi, Z., Di Pietro, F., Youssef, A. M., Reeves, J. M., Macey, P. M., Vickers, E. R., ... Henderson, L. A. (2016). Chronic neuropathic pain: It's about the rhythm. *The Journal of Neuroscience*, *36*(3), 1008–1018. <https://doi.org/10.1523/jneurosci.2768-15.2016>
- Antal, M., Beneduce, B. M., & Regehr, W. G. (2014). The Substantia Nigra conveys target-dependent excitatory and inhibitory outputs from the basal ganglia to the thalamus. *The Journal of Neuroscience*, *34*(23), 8032–8042. <https://doi.org/10.1523/JNEUROSCI.0236-14.2014>
- Apkarian, A. V., Sosa, Y., Sonty, S., Levy, R. M., Harden, R. N., Parrish, T. B., & Gitelman, D. R. (2004). Chronic back pain is associated with decreased prefrontal and thalamic gray matter density. *The Journal of Neuroscience*, *24*(46), 10410–10415. <https://doi.org/10.1523/JNEUROSCI.2541-04.2004>
- Ashburner, J. (2007). A fast diffeomorphic image registration algorithm. *NeuroImage*, *38*(1), 95–113. <https://doi.org/10.1016/j.neuroimage.2007.07.007>
- Ashburner, J., & Friston, K. J. (2009). Computing average shaped tissue probability templates. *NeuroImage*, *45*(2), 333–341. <https://doi.org/10.1016/j.neuroimage.2008.12.008>
- Baliki, M. N., Schnitzer, T. J., Bauer, W. R., & Apkarian, A. V. (2011). Brain morphological signatures for chronic pain. *PLoS One*, *6*(10), e26010. <https://doi.org/10.1371/journal.pone.0026010>
- Barad, M. J., Ueno, T., Younger, J., Chatterjee, N., & Mackey, S. (2014). Complex regional pain syndrome is associated with structural abnormalities in pain-related regions of the human brain. *The Journal of Pain*, *15*(2), 197–203.
- Becerra, L., Sava, S., Simons, L. E., Drosos, A. M., Sethna, N., Berde, C., ... Borsook, D. (2014). Intrinsic brain networks normalize with treatment in pediatric complex regional pain syndrome. *NeuroImage: Clinical*, *6*, 347–369.
- Behzadi, Y., Restom, K., Liao, J., & Liu, T. T. (2007). A component based noise correction method (CompCor) for BOLD and perfusion based fMRI. *NeuroImage*, *37*(1), 90–101. <https://doi.org/10.1016/j.neuroimage.2007.04.042>
- Bolwerk, A., Seifert, F., & Maihofner, C. (2013). Altered resting-state functional connectivity in complex regional pain syndrome. *The Journal of*

- Pain, 14(10), 1107–1115.e1108. <https://doi.org/10.1016/j.jpain.2013.04.007>
- Bourisly, A. K., El-Beltagi, A., Cherian, J., Gejo, G., Al-Jazzaf, A., & Ismail, M. (2015). A voxel-based morphometric magnetic resonance imaging study of the brain detects age-related gray matter volume changes in healthy subjects of 21–45 years old. *The Neuroradiology Journal*, 28(5), 450–459. <https://doi.org/10.1177/1971400915598078>
- Bultitude, J. H., Walker, I., & Spence, C. (2017). Space-based bias of covert visual attention in complex regional pain syndrome. *Brain*, 140(9), 2306–2321. <https://doi.org/10.1093/brain/awx152>
- Chou, Y. H., Chen, N. K., & Madden, D. J. (2013). Functional brain connectivity and cognition: Effects of adult age and task demands. *Neurobiology of Aging*, 34(8), 1925–1934. <https://doi.org/10.1016/j.neurobiolaging.2013.02.012>
- DaSilva, A. F., Becerra, L., Makris, N., Strassman, A. M., Gonzalez, R. G., Geatrakis, N., & Borsook, D. (2002). Somatotopic activation in the human trigeminal pain pathway. *The Journal of Neuroscience*, 22(18), 8183–8192.
- Erpelding, N., Simons, L., Lebel, A., Serrano, P., Pielech, M., Prabhu, S., ... Borsook, D. (2016). Rapid treatment-induced brain changes in pediatric CRPS. *Brain Structure & Function*, 221(2), 1095–1111. <https://doi.org/10.1007/s00429-014-0957-8>
- Farrell, M. J., Laird, A. R., & Egan, G. F. (2005). Brain activity associated with painfully hot stimuli applied to the upper limb: A meta-analysis. *Human Brain Mapping*, 25(1), 129–139. <https://doi.org/10.1002/hbm.20125>
- Friston, K. J., Holmes, A. P., Worsley, K. J., Poline, J. P., Frith, C. D., & Frackowiak, R. S. J. (1994). Statistical parametric maps in functional imaging: A general linear approach. *Human Brain Mapping*, 2(4), 189–210. <https://doi.org/10.1002/hbm.460020402>
- Geha, P. Y., Baliki, M. N., Harden, R. N., Bauer, W. R., Parrish, T. B., & Apkarian, A. V. (2008). The brain in chronic CRPS pain: Abnormal gray-white matter interactions in emotional and autonomic regions. *Neuron*, 60(4), 570–581. <https://doi.org/10.1016/j.neuron.2008.08.022>
- Gennatas, E. D., Avants, B. B., Wolf, D. H., Satterthwaite, T. D., Ruparel, K., Ciric, R., ... Gur, R. C. (2017). Age-related effects and sex differences in gray matter density, volume, mass, and cortical thickness from childhood to young adulthood. *The Journal of Neuroscience*, 37(20), 5065–5073. <https://doi.org/10.1523/jneurosci.3550-16.2017>
- Grady, C., Sarraf, S., Saverino, C., & Campbell, K. (2016). Age differences in the functional interactions among the default, frontoparietal control, and dorsal attention networks. *Neurobiology of Aging*, 41, 159–172. <https://doi.org/10.1016/j.neurobiolaging.2016.02.020>
- Gustin, S. M., Peck, C. C., Wilcox, S. L., Nash, P. G., Murray, G. M., & Henderson, L. A. (2011). Different pain, different brain: Thalamic anatomy in neuropathic and non-neuropathic chronic pain syndromes. *The Journal of Neuroscience*, 31(16), 5956–5964. <https://doi.org/10.1523/jneurosci.5980-10.2011>
- Gustin, S. M., Wrigley, P. J., Youssef, A. M., McIndoe, L., Wilcox, S. L., Rae, C. D., ... Henderson, L. A. (2014). Thalamic activity and biochemical changes in individuals with neuropathic pain after spinal cord injury. *Pain*, 155(5), 1027–1036. <https://doi.org/10.1016/j.pain.2014.02.008>
- Hashmi, J. A., Baliki, M. N., Huang, L., Baria, A. T., Torbey, S., Hermann, K. M., ... Apkarian, A. V. (2013). Shape shifting pain: Chronification of back pain shifts brain representation from nociceptive to emotional circuits. *Brain*, 136(9), 2751–2768. <https://doi.org/10.1093/brain/awt211>
- Henderson, L. A., Bandler, R., Gandevia, S. C., & Macefield, V. G. (2006). Distinct forebrain activity patterns during deep versus superficial pain. *Pain*, 120(3), 286–296. <https://doi.org/10.1016/j.pain.2005.11.003>
- Henderson, L. A., Peck, C. C., Petersen, E. T., Rae, C. D., Youssef, A. M., Reeves, J. M., ... Gustin, S. M. (2013). Chronic pain: Lost inhibition? *The Journal of Neuroscience*, 33(17), 7574–7582. <https://doi.org/10.1523/jneurosci.0174-13.2013>
- Hong, J. H., Kwon, H. G., & Jang, S. H. (2011). Probabilistic somatotopy of the spinothalamic pathway at the ventroposterolateral nucleus of the thalamus in the human brain. *AJNR. American Journal of Neuroradiology*, 32(7), 1358–1362. <https://doi.org/10.3174/ajnr.A2497>
- Hubbard, C. S., Becerra, L., Smith, J. H., DeLange, J. M., Smith, R. M., Black, D. F., ... Borsook, D. (2016). Brain changes in responders vs. non-responders in chronic migraine: Markers of disease reversal. *Frontiers in Human Neuroscience*, 10, 497. <https://doi.org/10.3389/fnhum.2016.00497>
- Kaas, J. H., Nelson, R. J., Sur, M., Dykes, R. W., & Merzenich, M. M. (1984). The somatotopic organization of the ventroposterior thalamus of the squirrel monkey, *Saimiri sciureus*. *The Journal of Comparative Neurology*, 226(1), 111–140. <https://doi.org/10.1002/cne.902260109>
- Kim, J. H., Choi, S. H., Jang, J. H., Lee, D. H., Lee, K. J., Lee, W. J., ... Kang, D. H. (2017). Impaired insula functional connectivity associated with persistent pain perception in patients with complex regional pain syndrome. *PLoS One*, 12(7), e0180479. <https://doi.org/10.1371/journal.pone.0180479>
- Kim, W., Kim, S. K., & Nabekura, J. (2017). Functional and structural plasticity in the primary somatosensory cortex associated with chronic pain. *Journal of Neurochemistry*, 141(4), 499–506. <https://doi.org/10.1111/jnc.14012>
- Kucyi, A., Hodaie, M., & Davis, K. D. (2012). Lateralization in intrinsic functional connectivity of the temporoparietal junction with salience- and attention-related brain networks. *Journal of Neurophysiology*, 108(12), 3382–3392. <https://doi.org/10.1152/jn.00674.2012>
- Lam, Y. W., & Sherman, S. M. (2011). Functional organization of the thalamic input to the thalamic reticular nucleus. *The Journal of Neuroscience*, 31(18), 6791–6799. <https://doi.org/10.1523/jneurosci.3073-10.2011>
- Lenz, F. A., Dostrovsky, J. O., Tasker, R. R., Yamashiro, K., Kwan, H. C., & Murphy, J. T. (1988). Single-unit analysis of the human ventral thalamic nuclear group: Somatosensory responses. *Journal of Neurophysiology*, 59(2), 299–316. <https://doi.org/10.1152/jn.1988.59.2.299>
- Low, A. K., Ward, K., & Wines, A. P. (2007). Pediatric complex regional pain syndrome. *Journal of Pediatric Orthopedics*, 27(5), 567–572.
- Lutz, J., Jager, L., de Quervain, D., Krauseneck, T., Padberg, F., Wichnalek, M., ... Schelling, G. (2008). White and gray matter abnormalities in the brain of patients with fibromyalgia: A diffusion-tensor and volumetric imaging study. *Arthritis and Rheumatism*, 58(12), 3960–3969. <https://doi.org/10.1002/art.24070>
- Maihofner, C., & Birklein, F. (2007). Complex regional pain syndromes: New aspects on pathophysiology and therapy. *Fortschritte der Neurologie-Psychiatrie*, 75(6), 331–342. <https://doi.org/10.1055/s-2006-944310>
- Maleki, N., Becerra, L., Brawn, J., Bigal, M., Burstein, R., & Borsook, D. (2012). Concurrent functional and structural cortical alterations in migraine. *Cephalalgia*, 32(8), 607–620. <https://doi.org/10.1177/0333102412445622>
- Manjon, J. V., Coupe, P., Marti-Bonmati, L., Collins, D. L., & Robles, M. (2010). Adaptive non-local means denoising of MR images with spatially varying noise levels. *Journal of Magnetic Resonance Imaging*, 31(1), 192–203. <https://doi.org/10.1002/jmri.22003>
- Moisset, X., & Bouhassira, D. (2007). Brain imaging of neuropathic pain. *NeuroImage*, 37(Suppl 1), S80–S88. <https://doi.org/10.1016/j.neuroimage.2007.03.054>
- Nagasaka, K., Takashima, I., Matsuda, K., & Higo, N. (2017). Late-onset hypersensitivity after a lesion in the ventral posterolateral nucleus of the thalamus: A macaque model of central post-stroke pain. *Scientific Reports*, 7(1), 10316. <https://doi.org/10.1038/s41598-017-10679-2>
- Penfield, W., & Boldrey, E. (1937). Somatic motor and sensory representation in the cerebral cortex of man as studied by electrical stimulation. *Brain: A Journal of Neurology*, 60, 389–443.
- Pinault, D. (2004). The thalamic reticular nucleus: Structure, function and concept. *Brain Research. Brain Research Reviews*, 46(1), 1–31. <https://doi.org/10.1016/j.brainresrev.2004.04.008>

- Power, J. D., Barnes, K. A., Snyder, A. Z., Schlaggar, B. L., & Petersen, S. E. (2012). Spurious but systematic correlations in functional connectivity MRI networks arise from subject motion. *NeuroImage*, 59(3), 2142–2154. <https://doi.org/10.1016/j.neuroimage.2011.10.018>
- Rajapakse, J. C., Giedd, J. N., & Rapoport, J. L. (1997). Statistical approach to segmentation of single-channel cerebral MR images. *IEEE Transactions on Medical Imaging*, 16(2), 176–186. <https://doi.org/10.1109/42.563663>
- Ralston, H. J., 3rd. (2005). Pain and the primate thalamus. *Progress in Brain Research*, 149, 1–10. [https://doi.org/10.1016/s0079-6123\(05\)49001-9](https://doi.org/10.1016/s0079-6123(05)49001-9)
- Rasmusson, D. (1996). Changes in the organization of the ventroposterior lateral thalamic nucleus after digit removal in adult raccoon. *The Journal of Comparative Neurology*, 364(1), 92–103. [https://doi.org/10.1002/\(SICI\)1096-9861\(19960101\)364:1<92::AID-CNE8>3.0.CO;2-N](https://doi.org/10.1002/(SICI)1096-9861(19960101)364:1<92::AID-CNE8>3.0.CO;2-N)
- Satterthwaite, T. D., Wolf, D. H., Loughhead, J., Ruparel, K., Elliott, M. A., Hakonarson, H., ... Gur, R. E. (2012). Impact of in-scanner head motion on multiple measures of functional connectivity: Relevance for studies of neurodevelopment in youth. *NeuroImage*, 60(1), 623–632. <https://doi.org/10.1016/j.neuroimage.2011.12.063>
- Shokouhi, M., Clarke, C., Morley-Forster, P., Moulin, D. E., Davis, K. D., & St Lawrence, K. (2017). Structural and functional brain changes at early and late stages of complex regional pain syndrome. *The Journal of Pain*, 19, 146–157. <https://doi.org/10.1016/j.jpain.2017.09.007>
- Simons, L. E., Pielech, M., Erpelding, N., Linnman, C., Moulton, E., Sava, S., ... Borsook, D. (2014). The responsive amygdala: Treatment-induced alterations in functional connectivity in pediatric complex regional pain syndrome. *Pain*, 155(9), 1727–1742. <https://doi.org/10.1016/j.pain.2014.05.023>
- Tohka, J., Zijdenbos, A., & Evans, A. (2004). Fast and robust parameter estimation for statistical partial volume models in brain MRI. *NeuroImage*, 23(1), 84–97.
- Van Dijk, K. R., Sabuncu, M. R., & Buckner, R. L. (2012). The influence of head motion on intrinsic functional connectivity MRI. *NeuroImage*, 59(1), 431–438. <https://doi.org/10.1016/j.neuroimage.2011.07.044>
- van Rijn, M. A., Marinus, J., Putter, H., Bosselaar, S. R. J., Moseley, G. L., & van Hilten, J. J. (2011). Spreading of complex regional pain syndrome: Not a random process. *Journal of Neural Transmission*, 118(9), 1301–1309. <https://doi.org/10.1007/s00702-011-0601-1>
- Verdugo, R. J., & Ochoa, J. L. (2000). Abnormal movements in complex regional pain syndrome: Assessment of their nature. *Muscle & Nerve*, 23(2), 198–205.
- Vukelic, M., Bauer, R., Naros, G., Naros, I., Braun, C., & Gharabaghi, A. (2014). Lateralized alpha-band cortical networks regulate volitional modulation of beta-band sensorimotor oscillations. *NeuroImage*, 87, 147–153. <https://doi.org/10.1016/j.neuroimage.2013.10.003>
- Walton, K. D., Dubois, M., & Llinas, R. R. (2010). Abnormal thalamocortical activity in patients with complex regional pain syndrome (CRPS) type I. *Pain*, 150(1), 41–51. <https://doi.org/10.1016/j.pain.2010.02.023>
- Whitfield-Gabrieli, S., & Nieto-Castanon, A. (2012). Conn: A functional connectivity toolbox for correlated and anticorrelated brain networks. *Brain Connectivity*, 2(3), 125–141. <https://doi.org/10.1089/brain.2012.0073>
- Willis, W. D. (1985). Nociceptive pathways: Anatomy and physiology of nociceptive ascending pathways. *Philosophical Transactions of the Royal Society of London. Series B, Biological Sciences*, 308(1136), 253–270.
- Woo, C. W., Krishnan, A., & Wager, T. D. (2014). Cluster-extent based thresholding in fMRI analyses: Pitfalls and recommendations. *NeuroImage*, 91, 412–419. <https://doi.org/10.1016/j.neuroimage.2013.12.058>
- Yamada, K., Nagakane, Y., Yoshikawa, K., Kizu, O., Ito, H., Kubota, T., ... Nishimura, T. (2007). Somatotopic organization of thalamocortical projection fibers as assessed with MR tractography. *Radiology*, 242(3), 840–845. <https://doi.org/10.1148/radiol.2423060297>
- Yeterian, E. H., & Pandya, D. N. (1989). Thalamic connections of the cortex of the superior temporal sulcus in the rhesus monkey. *The Journal of Comparative Neurology*, 282(1), 80–97. <https://doi.org/10.1002/cne.902820107>
- Youssef, A. M., Gustin, S. M., Nash, P. G., Reeves, J. M., Petersen, E. T., Peck, C. C., ... Henderson, L. A. (2014). Differential brain activity in subjects with painful trigeminal neuropathy and painful temporomandibular disorder. *Pain*, 155(3), 467–475. <https://doi.org/10.1016/j.pain.2013.11.008>

How to cite this article: Youssef AM, Azqueta-Gavaldon M, Silva KE, et al. Shifting brain circuits in pain chronicity. *Hum Brain Mapp.* 2019;40:4381–4396. <https://doi.org/10.1002/hbm.24709>